

# Photoproduction of $\Lambda(1520, 3/2^-)$

Seung-Il Nam,<sup>1, 2,\*</sup> Atsushi Hosaka,<sup>1, †</sup> and Hyun-Chul Kim<sup>2, ‡</sup>

<sup>1</sup>*Research Center for Nuclear Physics (RCNP),  
Osaka University, Ibaraki, Osaka 567-0047, Japan*

<sup>2</sup>*Department of physics and Nuclear physics & Radiation technology Institute (NuRI),  
Pusan University, Keum-jung gu, Busan 609-735, Korea*

## Abstract

We investigate the photoproduction of  $\Lambda(1520, 3/2^-)$  via the  $\gamma N \rightarrow K\Lambda^*$  reaction using the Born approximation and the Rarita-Schwinger vector-spinor field for the spin 3/2 particle. We reproduce the experimental data of the total cross section and the angular dependence for the proton target qualitatively well and estimate them for the neutron target. For the neutron target, we find much smaller total cross section than that of the proton and the significant  $K^*$ -exchange contribution.

PACS numbers: 13.75.Cs, 14.20.-c

Keywords:  $\Lambda(1520)$ , spin 3/2, photoproduction

---

\*Electronic address: sinam@rcnp.osaka-u.ac.jp

†Electronic address: hosaka@rcnp.osaka-u.ac.jp

‡Electronic address: hchkim@pusan.ac.kr

## I. INTRODUCTION

After the observation of the pentaquark baryon  $\Theta^+(1540)$  [1], the  $\Theta^+$  baryon has been one of the most interesting issues among the recent studies for the hadron systems. Taking into account the fact that the LEPS collaboration found that  $\Lambda(1520)$  is produced simultaneously in the  $\Theta^+$  photoproduction on the deuteron, it is of great importance to study on the producing mechanism of the  $\Lambda(1520)$  and of  $\Theta^+$  on the same footing. Therefore, in the present report, we present a recent investigation on the photoproduction of  $\Lambda^*$  ( $\equiv \Lambda(1520)$ ) via  $\gamma N \rightarrow K\Lambda^*$  using the Born approximation. In order to consider the spin 3/2 baryon relativistically, we employ the Rarita-Shwinger vector-spinor field formalism [2]. Though the theoretical calculation contains several model parameters, we observe that the model-parameter dependences are rather weak in the low energy region, where the Born approximation works appropriately. We also find that the contact term contribution is dominant over other channels.

As for the  $\Lambda^*$  photoproduction on the proton target, we can reproduce qualitatively well the experimental data [3], the total cross section and the angular dependence, using the four dimensional gauge invariant formfactor [4]. We also observe that the angular distribution demonstrates a strong enhancement in forward scattering, which agrees well with the experimental data.

In the case of the neutron target, the order of magnitude of the total cross section is much smaller than that of the proton one, since the contact term does not exist in the neutron case. However, in this case, being different from the proton case,  $K^*$ -exchange contributes much to the angular distribution which shows a peak around  $45^\circ$ .

We will organize the present report as follows. In Section II we briefly introduce the formalism used in the present report. We will demonstrate the numerical results in Section III. Finally we summarize the present work.

## II. GENERAL FORMALISM

We start with the relevant Lagrangians for the interaction vertices in the  $\gamma N \rightarrow K\Lambda^*$  reaction.

$$\mathcal{L}_{\gamma NN} = -e\bar{p} \left( \gamma_\mu + i\frac{\kappa_p}{2M_p} \sigma_{\mu\nu} k_1^\nu \right) A^\mu N + \text{h.c.},$$

$$\begin{aligned}
\mathcal{L}_{\gamma K K} &= ie \left\{ (\partial^\mu K^\dagger) K - (\partial^\mu K) K^\dagger \right\} A_\mu + \text{h.c.}, \\
\mathcal{L}_{\gamma \Lambda^* \Lambda^*} &= -\bar{\Lambda}^{*\mu} \left\{ \left( -F_1 \not{g}_{\mu\nu} + F_3 \not{g} \frac{k_{1\mu} k_{1\nu}}{2M_{\Lambda^*}^2} \right) - \frac{\not{k}_1 \not{\ell}}{2M_{\Lambda^*}} \left( -F_2 g_{\mu\nu} + F_4 \frac{k_{1\mu} k_{1\nu}}{2M_{\Lambda^*}^2} \right) \right\} \Lambda^{*\nu} + \text{h.c.}, \\
\mathcal{L}_{\gamma K K^*} &= g_{\gamma K K^*} \epsilon_{\mu\nu\rho} (\partial^\mu A^\nu) (\partial^\rho K) K^{*\rho} + \text{h.c.}, \\
\mathcal{L}_{K N \Lambda^*} &= \frac{g_{K N \Lambda^*}}{M_K} \bar{\Lambda}^{*\mu} \Theta_{\mu\nu}(A, Z) (\partial^\nu K) \gamma_5 p + \text{h.c.}, \\
\mathcal{L}_{K^* N \Lambda^*} &= -\frac{ig_{K^* N \Lambda^*}}{M_V} \bar{\Lambda}^{*\mu} \gamma^\nu (\partial_\mu K_\nu^* - \partial_\nu K_\mu^*) p + \text{h.c.}, \\
\mathcal{L}_{\gamma K N \Lambda^*} &= -i \frac{eg_{K N \Lambda^*}}{M_K} \bar{\Lambda}^{*\mu} A_\mu K \gamma_5 N + \text{h.c.}
\end{aligned} \tag{1}$$

Here,  $N$ ,  $\Lambda_\mu^*$ ,  $K$  and  $A^\mu$  are the nucleon,  $J = 3/2^-$  Rarita-Schwinger spinor for  $\Lambda^*$ , pseudo-scalar kaon and photon fields, respectively. In order to maintain the gauge invariance for the present reaction, the contact term (Kroll-Ruderman term) is necessary. The interaction for the  $K^* N \Lambda^*$  vertex is taken from Ref. [5]. As for the  $\gamma \Lambda^* \Lambda^*$  vertex in the  $u$ -channel, we utilize the effective interaction suggested by Ref. [6] which contains four terms related to the electric and magnetic multipoles. We will ignore the electric coupling  $F_1$ , since the  $\Lambda^*$  is neutral. We will also neglect  $F_3$  and  $F_4$  terms, assuming that higher multipole terms are less important. Hence, for the photon coupling to  $\Lambda^*$ , we consider only the magnetic coupling term  $F_2$  whose strength is proportional to the anomalous magnetic moment of  $\Lambda^*$ ,  $\kappa_{\Lambda^*}$ , will be treated as a free parameter.  $\Theta_{\mu\nu}(A, Z)$  containing the off-shell contribution of the spin-3/2 particle is defined as  $\Theta_{\mu\nu}(X) = g_{\mu\nu} + X \gamma_\mu \gamma_\nu$  in which  $X$  is the reduced off-shell parameter [7] and will be also treated as a free parameter.

In order to determine the coupling constant  $g_{K N \Lambda^*}$  we make use of the decay width  $\Gamma_{\Lambda^* \rightarrow K N} = 15.6$  MeV with decay ratio 0.45 [8]. We obtain  $g_{K N \Lambda^*} = 11.075$ . As for the  $K^* N \Lambda^*$  coupling constant, we will choose the values of 0,  $\pm g_{K N \Lambda^*}$  and  $\pm 2g_{K N \Lambda^*}$  for the numerical calculation, since we have no information on how to determine the coupling constant. The coupling constant of  $g_{\gamma K^* K}$  is taken to be 0.254/GeV for the charged decay and 0.388/GeV for the neutral decay [8]. As suggested in Ref. [4], we adopt the following parameterization for the four dimensional form factors satisfying the crossing symmetry:

$$\begin{aligned}
F_x(q^2) &= \frac{\Lambda^4}{\Lambda^4 + (x - M_x^2)^2}, \quad x = s, t, u, v \\
F_c &= F_s + F_t - F_s F_t.
\end{aligned} \tag{2}$$

The form of  $F_c$  is chosen in such a way that the on-shell values of the coupling constants are reproduced.

### III. NUMERICAL RESULTS

First, we present the numerical results of the total cross sections for the proton target using several different model parameter sets in Fig. 1. In the figures, we change the model parameters for  $-1 < \kappa_{\Lambda^*} < 1$ ,  $-1 < X < 1$  and  $-22.14 < g_{K^*N\Lambda^*} < 22.14$  in order to see the dependence on the model parameters. The experimental data is taken from Ref. [3]. Though the curves demonstrate sizable model parameter dependences in the higher energy region but the dependences become rather weak in the low energy region, where the Born approximation is known to work well. We note that the total cross section for the proton target shows the  $S$ -wave threshold behavior ( $\sim [E_{\text{th}} - E_{\gamma}]^{1/2}$ ) due to the contact term contribution. Within the several parameter sets, we choose  $\kappa_{\Lambda^*} = -0.5$ ,  $X = 0$  and  $g_{K^*N\Lambda^*} = 0, \pm g_{K^*N\Lambda^*}$  which reproduce the data relatively well for the numerical calculations.

In Fig. 2, we show the  $t$ -dependence for the chosen parameter sets. The experimental data are also taken from Ref. [3]. The experimental values are averaged ones for the incident photon lab energy range from 2.8 GeV to 4.8 GeV. We plot the momentum-transfer dependence for energies in the COM. For  $E_{\text{CM}} = 2.4$  GeV, 2.7 GeV and 3.0 GeV which lie in the incident photon lab energy range, we can reproduce the data qualitatively well. We observe that the numerical results for the momentum transfer dependence is not sensitive to the model parameters and indicates the strong enhancement in the forward scattering. The backward scattering is suppressed due to the four dimensional formfactor  $F_c$  in Eq. (2).

Turning to the neutron target case in Fig. 3, we show the total cross sections with the model parameters which are determined in the proton target case. We observe that results increase drastically beyond  $E_{\gamma\text{lab}} \gtrsim 3.0$  GeV. We confirm that this unnatural behavior comes from the  $u$ -channel contribution which contains the model parameters  $\kappa_{\Lambda^*}$  and  $X$ . The threshold behavior is strongly dependent on the inclusion of the vector  $K^*$ -exchange contribution. Since the contact term, which is the largest contribution among the kinematical channels, does not exist in the neutron target case, the order of magnitude of the total cross section is much smaller than that of the proton case.

Finally, In Fig. 4 we demonstrate the angular dependences on the parameter sets. The peaks at  $\sim 45^\circ$  in these figures indicate that the  $K^*$ -exchange contributes significantly to the  $\Lambda^*$  photoproduction reaction on the neutron target. This  $K^*$ -exchange dominant behavior was also shown in the  $\gamma p \rightarrow \bar{K}^0 \Theta^+$  reaction, in which the  $K^*$ -exchange is the only  $t$ -channel

contribution [9].

#### IV. SUMMARY

We have studied the  $\Lambda(1520)$  photoproduction in the Born approximation. The physical observables, the total cross sections, and the angular dependence were calculated with appropriate model parameters used. The model parameter dependences were not so strong in the low energy region. We were able to reproduce the experimental data qualitatively well for the proton target and estimate the total and differential cross sections for the neutron one which has not been measured yet. We observed that the contact term contribution is the largest one among the kinematical channels. Therefore, the absence of the contact term in the neutron target case makes the total cross section much smaller than that of the proton. We also note  $K^*$ -exchange plays a significant role in the case of the neutron target. The more detailed work on the photoproduction of  $\Lambda^*$  is under way [10].

#### Acknowledgement

We thank T. Nakano and A. Titov for fruitful discussions and comments. The work of S.I.N. has been supported by the scholarship endowed from the Ministry of Education, Science, Sports, and Culture of Japan. The work of H.C.K. is supported by the Korean Research Foundation (KRF-2003-070-C00015).

---

- [1] T. Nakano *et al.* [LEPS Collaboration], Phys. Rev. Lett. **91**, 012002 (2003).
- [2] W. Rarita and J. S. Schwinger, Phys. Rev. **60**, 61 (1941).
- [3] D. P. Barber *et al.*, Z. Phys. C **7**, 17 (1980).
- [4] R. M. Davidson and R. Workman, arXiv:nucl-th/0101066.
- [5] R. Machleidt, K. Holinde and C. Elster, Phys. Rept. **149**, 1 (1987).
- [6] M. Gourdin, Nuovo Cimento **36**, 129 (1965); and, **40A**, 225 (1965).
- [7] B. J. Read, Nucl. Phys. B **52**, 565 (1973).
- [8] S. Eidelman *et al.* [Particle Data Group], Phys. Lett. B **592**, 1 (2004).
- [9] S. I. Nam, A. Hosaka and H. C. Kim, arXiv:hep-ph/0403009.

[10] S. I. Nam, A. Hosaka and H. C. Kim, in preparation.

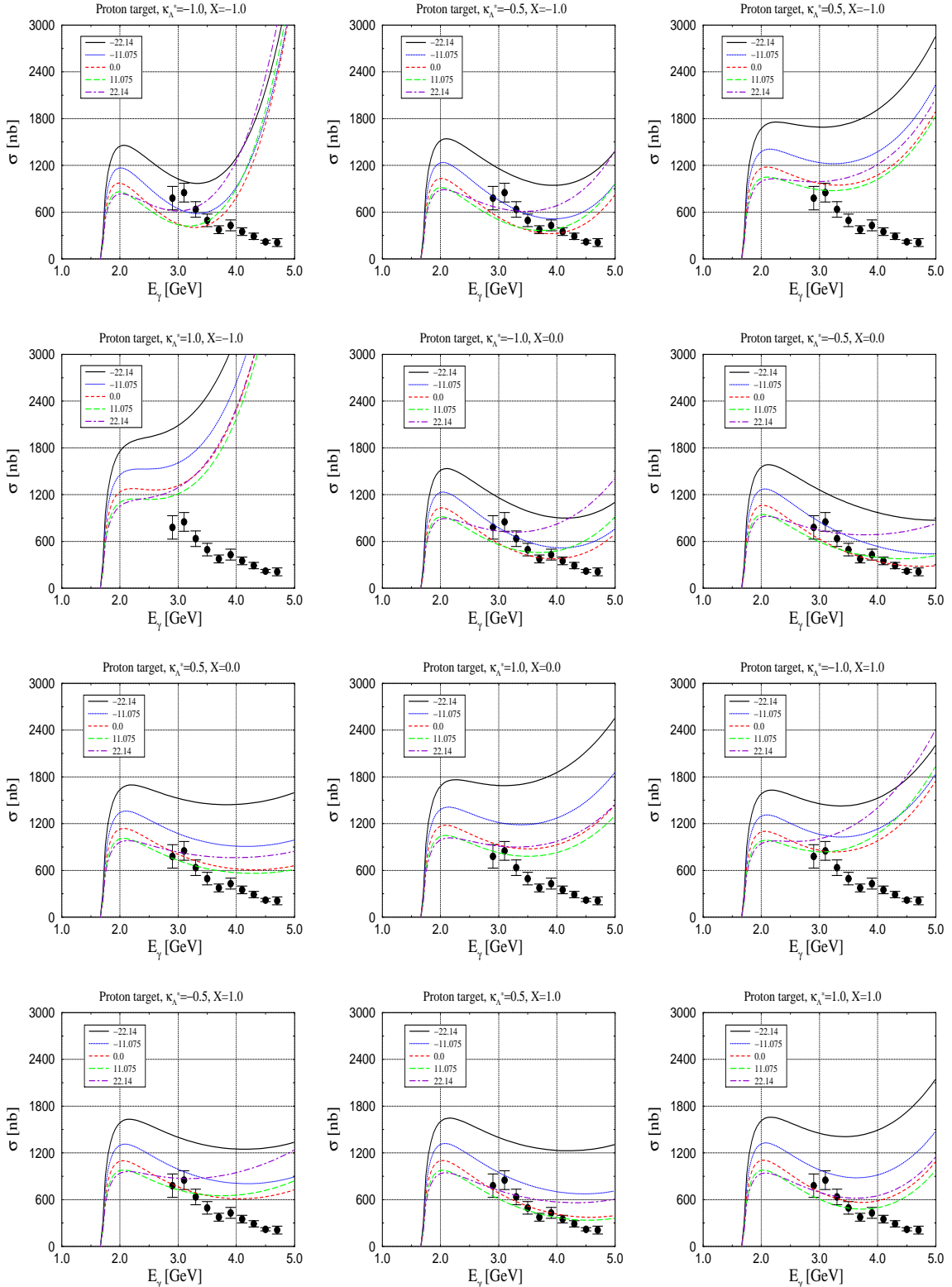


FIG. 1: The total cross sections for the proton target by changing the model parameters which are  $\kappa_{\Lambda^*}$ ,  $X$  and  $g_{K^*N\Lambda^*}$ .

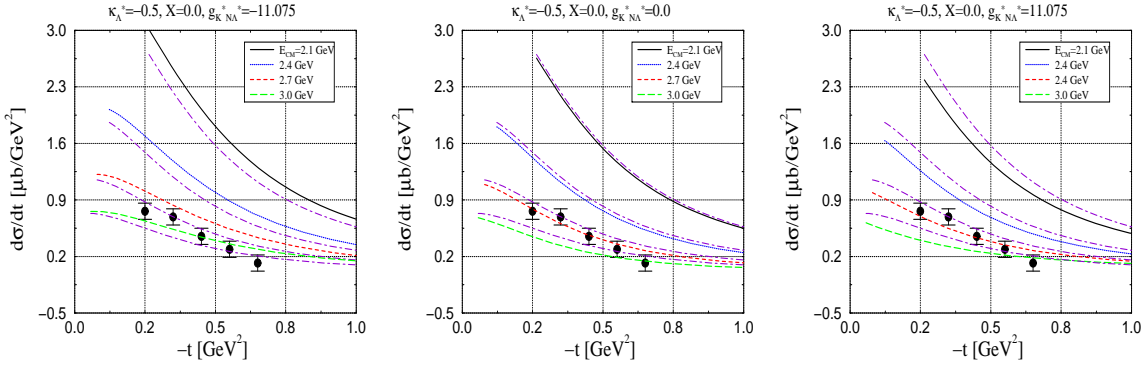


FIG. 2: The momentum transfer dependence for the proton target changing the model parameters which are  $\kappa_{\Lambda^*}$ ,  $X$  and  $g_{K^*NA^*}$ . Dot-dashed lines indicated the case without the model parameters.

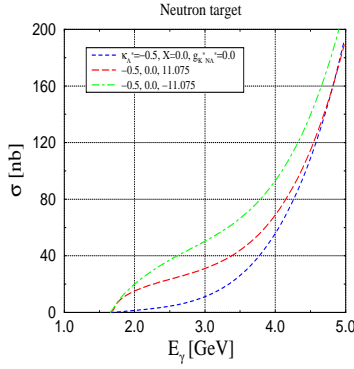


FIG. 3: The total cross sections for the neutron target changing the model parameters.

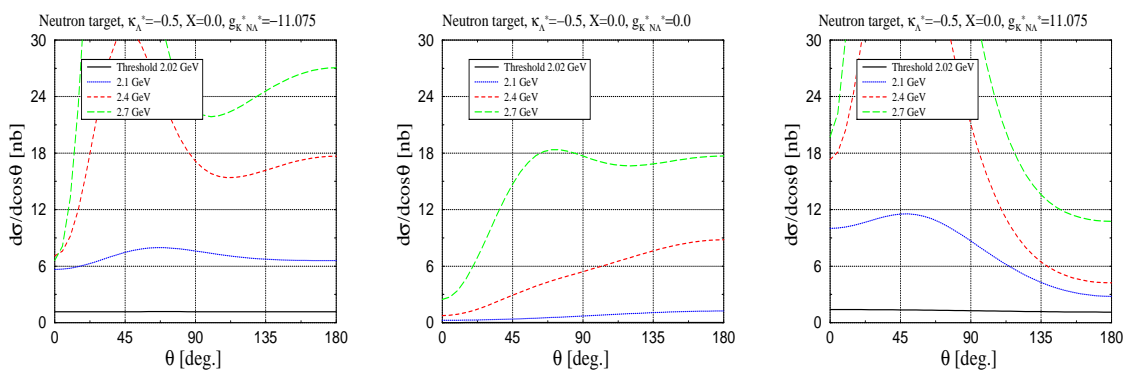


FIG. 4: The angular distributions for the neutron target with the parameter sets.